Carbohydrate Polymers 105 (2014) 207–213

Contents lists available at ScienceDirect

Carbohydrate Polymers

journal homepage: www.elsevier.com/locate/carbpol

Thermoset nanocomposites from two-component waterborne polyurethanes and cellulose whiskers

Guo-min Wu[a,b,*], Jian Chen[a], Shu-ping Huo[a], Gui-feng Liu[a,b], Zhen-wu Kong[a,b]

[a] Institute of Chemical Industry of Forest Products, Chinese Academy of Forestry; Key Laboratory of Biomass Energy and Material of Jiangsu Province; Key and Open Laboratory on Forest Chemical Engineering, State Forestry Administration; National Engineering Laboratory for Biomass Chemical Utilization, Nanjing 210042, China
[b] Research Institute of New Technology, Chinese Academy of Forestry, Beijing 10091, China

ARTICLE INFO

Article history:
Received 19 November 2013
Received in revised form 8 January 2014
Accepted 21 January 2014
Available online 5 February 2014

Keywords:
Two-component waterborne polyurethanes
Cellulose nanowhiskers
Nanocomposite
Turpentine

ABSTRACT

We prepared thermoset nancomposites from biomass-based two-component waterborne polyurethane (2K-WPU) and cellulose namowhiskers (CNWs). Due to the formation of hydrogen bonds, the viscosity of 2K-WPU dispersion was found to be increased with the addition of CNWs. SEM images showed "sea-island structure" corresponding to the microphase separation between CNWs nano-filler and the 2K-WPU matrix. The α-relaxation temperature (T_α) and glass transition temperature (T_g) increased with the increase of CNWs content, which was due to the formation of a rigid CNWs nano-phase acting as crosslinking points in the 2K-WPU matrix. Mechanical properties from tensile test showed Young's modulus and tensile strength of 2K-WPU/CNWs nanocomposites were reinforced by the addition of CNWs. Thermo-stability of 2K-WPU/CNWs nanocomposites decreased slightly with the increase of CNWs content, which could be attributed to the increased thermal conductivity of the material after adding CNWs.

1. Introduction

Given the good mechanical properties of solvent-based two-component polyurethane systems, they have been successfully used in various applications, e.g. coatings, adhesives. During the past decades, reduction of volatile organic compounds (VOCs) emissions has become the major driving force of resin developments. One approach of reducing VOCs emissions during resin industry is substituting solvent-based systems by waterborne systems. Two-component waterborne polyurethanes (2K-WPUs) which combine the environment-friendly property of waterborne resins with the good performance of two-component polyurethanes have been developed for a number of industrial applications (Chang & Lu, 2012; Melchiors, Sonntag, & Kobusch, 2000; Otts & Urban, 2005; Otts, Pereira, Arret, & Urban, 2005; Wicks, Wicks, & Rosthauser, 2002). However, unlike the homogeneous film formation of solvent-based two-component polyurethane systems, the film formation of 2K-WPUs is a heterogeneous phase process among water-dispersed particles. The mechanical properties of the film of 2K-WPUs are not as good as that of solvent-based two-component system. It is necessary to strengthen the mechanical properties of 2K-WPUs at the molecular level by chemical (Ge & Luo, 2013) or composite modification methods (Akbarian, Olya, Ataeefard, & Mahdavian, 2012).

Recent researches have shown that the properties of polymer resins could be further improved by the addition of particles in the nanoscale range (Alexandre & Dubois, 2000). The nanocomposites exhibit improved mechanical properties and can improve resistance to moisture and weathering. More recently, cellulose nanowhiskers (CNWs) have been considered as potential reinforcing agents for polymer-based composite materials (Eichorn et al., 2010; Favier, Chanzy, & Cavaillé, 1995; Jacob & Thomas, 2008; Klemm et al., 2011). Cellulose in plants consists of 1,4-β-glucopyranose units associated by hydrogen bonding. It forms a semicrystalline structure where highly ordered regions (the crystallites) are distributed among disordered domains (the amorphous phase). Cellulose crystallites are in nanometer size and can be obtained by various well-documented methods (Abdul Khalil, Bhat, & Ireana Yusra, 2012; Azizi Samir, Alloin, & Dufresne, 2005; Hubbe, Rojas, Lucia, & Sain, 2008; Souza Lima & Borsali, 2004). Because of their high specific strength, modulus, and aspect ratio, they can significantly improve the mechanical properties of composites at

* Corresponding author at: Institute of Chemical Industry of Forest Products, Chinese Academy of Forestry; Key Laboratory of Biomass Energy and Material of Jiangsu Province; Key and Open Laboratory on Forest Chemical Engineering, State Forestry Administration; National Engineering Laboratory for Biomass Chemical Utilization, Nanjing 210042, China. Fax: +86 2585482457.
E-mail address: woogm@hotmail.com (G.-m. Wu).

0144-8617/$ – see front matter © 2014 Elsevier Ltd. All rights reserved.
http://dx.doi.org/10.1016/j.carbpol.2014.01.095

loading levels as low as 5%. Other advantages of nanocrystals stem from their low density, renewable nature, biodegradability, and relatively low cost.

In order to realize property improvements, CNWs must be homogeneously dispersed in polymeric matrix. Given the high surface area and hydrophilic nature, CNWs are well dispersed in water, but difficult to be dispersed in solvent-based resins (Pu et al., 2007; Qua, Hornsby, Sharma, Lyons, & McCall, 2009; Roohani et al., 2008). One method to overcome this problem is chemically modifying the surface of the CNWs by appropriate functions, so that the polar hydroxyl groups can be converted to moieties which modifies the fiber wettability and enhances the interaction of CNWs with the matrix (Çetin et al., 2009; Habibi et al., 2008; Siqueira, Bras, & Dufresne, 2010; Stenstad, Andresen, Tanem, & Stenius, 2008). However, the chemical strategies of surface modification of CNWs are quite inefficient. It is difficult to efficiently reinforce most of the classical resin matrices. Since stable suspensions of CNWs can be easily prepared in water, their incorporation in waterborne resin to prepare cellulose nanocomposites is an efficient strategy for the utilization of CNWs without modification. So far, CNWs have been reported to be filled into thermoplastic one-component waterborne polyurethanes, resulting in a significant increase of strength and Young's modulus (Cao, Dong, & Li, 2007; Lee & Kim, 2012; Oliveira Patricio et al., 2013; Zou et al., 2011).

As an abundant carbon-neutral renewable resource and a viable supplement to fossil fuel resources, biomass is gaining extensive research attention for producing energy and materials. In our previous work, a biomass-based 2K-WPU was prepared by a polyol (WPOL) dispersion from the raw material turpentine and a hydrophilically modified hexamethylene diisocyanate (HDI) tripolymer (Wu et al., 2013). Different from the particle merging mechanism of the film formation of one-component waterborne polyurethanes, the film formation process of 2K-WPU contains not only particle merging but also crosslinking reaction between different components. In this work, we prepared novel 2K-WPU/CNWs nanocomposites by incorporating CNWs suspension, which was hydrolyzed from microcrystalline cellulose (MCC), into the biomass-based 2K-WPU. The abundant active hydroxyl groups on the surface of CNWs can take part in the crosslinking reaction with isocyanate groups of HDI, resulting in strong interfacial adhesion between the matrix and the filler. The crosslinking reaction, structure, and properties of the prepared nanocomposite materials were investigated by rotational rheometer, scanning electron microscopy (SEM), differential scanning calorimetry (DSC), thermogravmetric analysis (TGA), dynamic mechanical analysis (DMA), and tensile tests.

2. Experimental

2.1. Materials

Terpinene-maleic ester type epoxy resin (TME) was synthesized from raw material turpentine (Wu, Kong, Huang, Chen, & Chu, 2007). It is an alicyclolic epoxy resin with endocyclic structure and has an epoxy value of 3.5 mmol g^{-1}. Polyethylene glycol (PEG) (M_n = 4000) was purchased from Guangdong Xilong Chemical Co., Ltd., China. Trimethylolpropane (TMP) and microcrystalline cellulose (MCC) were purchased from Aladdin Industrial Co., China. Boron fluoride ethyl ether was supplied by Shanghai Lingfeng Chemical Reagent, Co., Ltd., China. Acetone was obtained from Nanjing Chemical Reagent, Co., Ltd., China. The hydrophilically modified HDI tripolymer with NCO content of 13 wt% and solid content of 80 wt%, was supplied by Wuhan Shiquanshi Decorative Coating Co., Ltd., China. Sulfuric acid (H_2SO_4) was purchased from Sinopharm Chemical Reagent Co., Ltd., China.

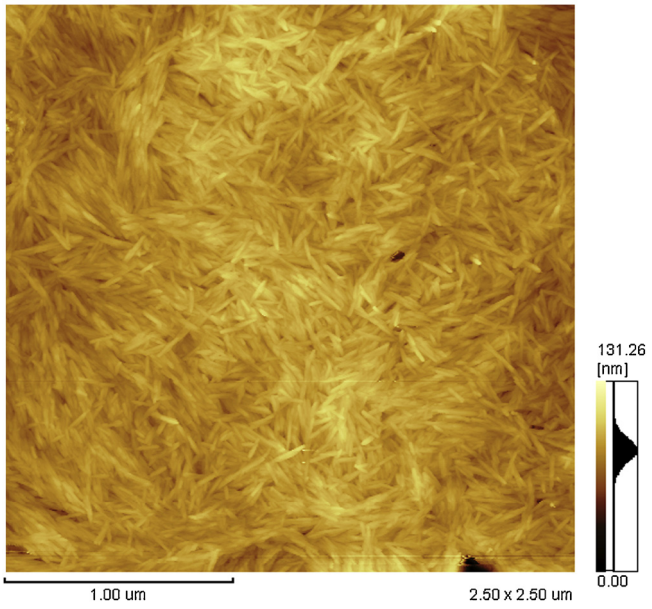

Fig. 1. AFM image of CNWs.

2.2. Preparation of WPOL and WPOL dispersion

The synthesis of WPOL has been described in details in our previous work (Wu, Kong, Chen, & Jiang, 2011), and therefore only a brief description follows. A 500 ml four-necked flask equipped with stirrer, dropping funnel, thermometer, condenser, and heating mantle was charged with 86.6 g TME, 15.6 g PEG and 14.5 g TMP. After the temperature inside the flask increased to 90 °C, 0.87 g boron fluoride ethyl ether diluted in 6.1 g acetone was added with constant stirring. The reaction was continued for 1.5 h at 110–120 °C, producing a yellow transparent product WPOL. By churning at 500–1000 rpm, at 50–90 °C, 210 g distilled water was added slowly to disperse the produced WPOL, generating a milk-white dispersion (WPOL dispersion) with 35 wt% solid content.

2.3. Preparation of CNWs

CNWs were prepared according the reported studies (Bondeson, Mathew, & Oksman, 2006). 10.0 g MCC was mixed with 110 ml sulfuric acid solution (63.5 wt%). The mixture was stirred vigorously for 2 h at 44 °C. The formed suspension was diluted with 500 g distilled water to stop the reaction. Then the suspension was repeatedly centrifuged and washed with distilled water. Dialysis was performed to remove the residual acid in the suspension. After concentrated under vacuum and adjusted with distilled water, a stable CNWs suspension with solid content of 3.0 wt% was obtained through 30 min ultrasonic treatment. The stereoscopic information of the CNWs collected with an atomic force microscope (AFM) is shown in Fig. 1. The rod-like CNWs are observed having the width of 20–40 nm and the length of 200–300 nm.

2.4. Preparation of 2K-WPU/CNWs nanocomposite films

CNWs suspension was mixed with the WPOL dispersion under sonication for 10 min. Then the mixture was blended with hydrophilically modified HDI tripolymer at a hydroxyl group to isocyanate group molar ratio of 1:1.2. The generated blend called 2K-WPU/CNWs dispersion was first diluted with distilled water to the solid content of 30 wt%, and then degassed under vacuum at ambient temperature. Subsequently, the 2K-WPU/CNWs dispersion was cast in square Teflon molds and dried at 30 °C for 1 week.

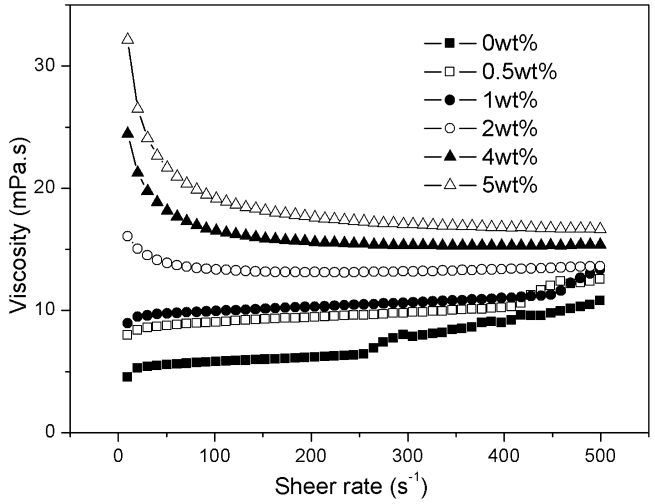

Fig. 2. Effect of CNWs content on the rheological properties of 2K-WPU/CNWs dispersions.

By altering the content of CNWs in the range of 0, 0.5, 1, 2, 3, 4, 5 wt% w.r.t. 2K-WPU, a series of nanocomposite films with a thickness of approximately 0.5 mm were obtained, and denoted as 0 wt%, 0.5 wt%, 1 wt%, 2 wt%, 3 wt%, 4 wt%, and 5 wt%, respectively.

2.5. Characterizations

AFM image of CNWs was taken by a SPM9600 atomic force microscope (Shimadzu, Japan) in phase mode. To prepare the AFM sample, a droplet of CNWs suspension was coated on a silicon substrate, and dried under vacuum for 12 h. The AFM image was recorded in height trace.

Rheological properties of 2K-WPU/CNWs dispersions (30 wt% solid content) were investigated by a Haake Mars-III rotational rheometer (Thermo Scientific, Germany) using coaxial cylinder technique. The shear rates ranged from 0 s^{-1} to 500 s^{-1}.

The crosslinking behaviors of 2K-WPU/CNWs were investigated by a Haake Mars-III rotational rheometer (Thermo Scientific, Germany) in a cone-plate geometry (diameter of 25 mm, gap of 0.5 mm). Oscillatory measurements which allow the monitoring of viscoelastic properties (i.e. viscosity, storage modulus G', and loss modulus G'') during the crosslinking process of 2K-WPU/CNWs were performed with a temperature sweep range of 20–150 °C at a rate of 2 K min^{-1} and at 150 °C for 30 min. The oscillation frequency was 2 Hz.

Cross-section micrographs of the nanocomposite films were obtained by scanning electron microscopy (SEM) (Hitach S3400N, Japan) at 15 kV. The films were frozen in liquid nitrogen and snapped immediately.

DSC analysis was carried out on a PerkinElmer Diamond differential scanning calorimeter (USA) at heating rate of 20 K min^{-1} and nitrogen gas flow of 20 ml min^{-1}. The specimens were crimple-sealed in aluminum crucibles and scanned from −50 °C to 150 °C.

TGA was conducted on a NETZSCH STA 409 PC/PG thermogravimetric analyzer (Germany). The samples were placed in an aluminum pan and heated in nitrogen atmosphere from 25 °C to 600 °C at heating rate of 10 K min^{-1}.

DMA was carried out on a Q800 dynamic mechanical analyzer (TA instrument, USA) at frequency of 1 Hz, temperature range of −50 to 150 °C, and heating rate of 2 K min^{-1}. The size of the specimens cut from the nanocomposite films was 40 mm × 6.5 mm × 0.5 mm.

The tensile tests of the nanocomposite films were conducted on a universal testing machine (CMT4304, Shenzhen SANS, China)

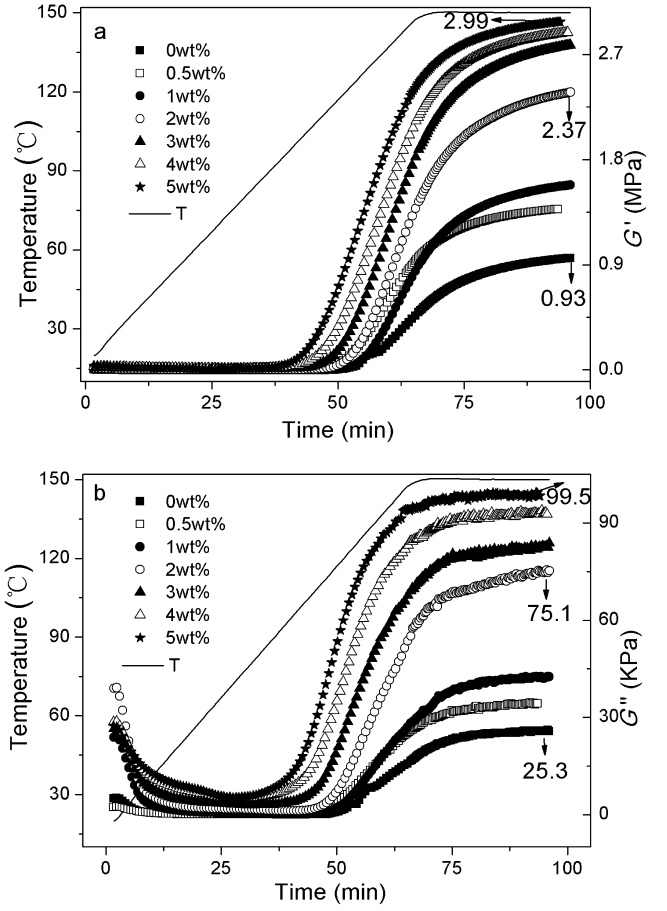

Fig. 3. Variation of the storage modulus (G') (a) and the loss modulus (G'') (b) during the crosslinking process of 2K-WPU/CNWs.

at loading rate of 100 mm min^{-1} according to the ASTM D412 standard at room temperature. For each specimen, we took average value from five replicates.

3. Results and discussion

3.1. Rheological properties of 2K-WPU/CNWs dispersions

The active hydroxyl groups on the surface of CNWs can form hydrogen bonds with the dispersion medium (water) and the macromolecular chains of resins. This can increase the viscosity of the waterborne resin dispersions (Matos Ruiz, Cavaille, Dufrense, Graillat, & Gerard, 2001). Fig. 2 shows the influence of CNWs content on the rheological properties of 2K-WPU/CNWs dispersions at room temperature. Due to the formation of hydrogen bonds, the viscosity of 2K-WPU/CNWs dispersion increases with the increase of CNWs content. The shear viscosities of 2K-WPU/CNWs dispersions are low when the CNWs content is lower than 2 wt%. They increase with the increase of shear rate and show a characteristic of dilatant fluid. This is because the dispersed phase of the dispersion becomes more disorder and accounts for larger volume when the shear stress increases. However, when the CNWs content is more than 2 wt%, the shear viscosities of the dispersions decrease with the increase of shear rate and show a characteristic of pseudoplastic fluid. The change of the rheological property of 2K-WPU/CNWs dispersion with the CNWs content can be attributed to the formation and break-up of hydrogen bonds in the dispersion. More hydrogen bonds are formed in the dispersion with the increase of CNWs content, which results in higher viscosity of the dispersion. When the

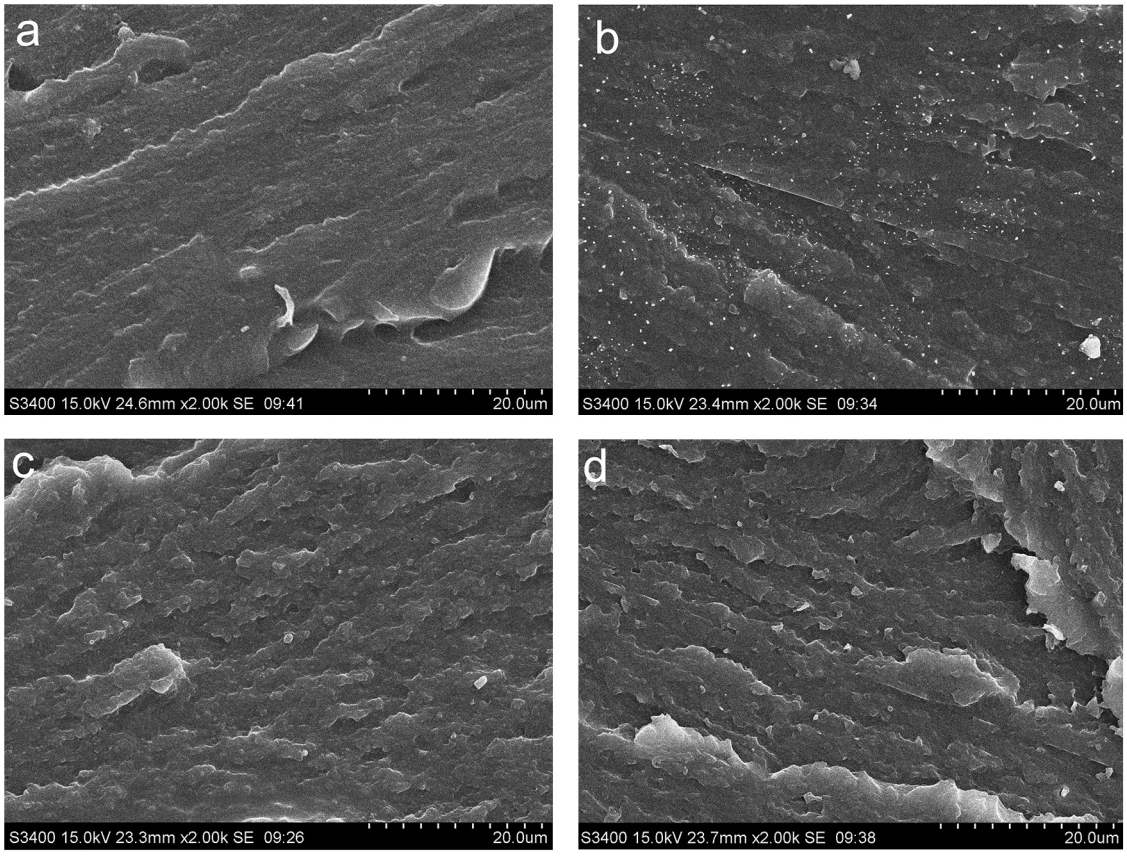

Fig. 4. SEM images of 2K-WPU/CNWs nanocomposite films with different CNWs contents, 0 wt% (a), 1 wt% (b), 2 wt% (c) and 4 wt% (d) (scale bar: 20 um).

shear stress is increased, the hydrogen bonds can be broken and the dispersion shows shear thinning.

3.2. Crosslinking process of 2K-WPU/CNWs dispersions

The storage modulus (G') and the loss modulus (G'') during the crosslinking process of 2K-WPU/CNWs with different CNWs contents are shown in Fig. 3. During the temperature-rise period, G' and G'' undergo a decrease followed by a fast increase. With the temperature rising, the viscosities of 2K-WPU/CNWs would decrease, leading to a fall of G' and G''. However, G' and G'' rise fast when the crosslinking reaction between hydroxyl groups and isocyanate groups take place. At constant temperature of 150 °C, G' and G'' rise slowly and keep stable afterwards, which indicates the complete crosslinking of the reaction. With the increase of CNWs content, simultaneous enhancements of G' and G'' are found for all 2K-WPU/CNWs nanocomposites. At the end of the crosslinking reaction, the enhancements of G' and G'' are proportional to the CNWs contents in the range of 0–5 wt%. As shown in Fig. 3, for 2K-WPU/CNWs nanocomposite containing 2 wt% CNWs, G' and G'' are 155% and 197%, respectively, and in the condition of 5 wt% CNWs, G' and G'' are 222% and 293%, respectively, higher than those of neat 2K-WPU (0 wt%). The simultaneous enhancement of G' and G'' can be attributed to the well homodispersion of the CNWs in nano-scale (Chen et al., 2008) as well as the increase of physical interaction and chemical grafting between CNWs nano-filler and the 2K-WPU matrix.

3.3. Morphology of 2K-WPU/CNWs nanocomposite films

Fig. 4 shows the SEM images of the fractured surfaces of 2K-WPU/CNWs nanocomposite films. Compared to the micrograph of neat 2K-WPU (0 wt%), more "sea-island structures" appear in the micromorphology of 2K-WPU/CNWs nanocomposite films with the increase of CNWs content. The formation of "sea-island structure" could correspond to the microphase separation between the CNWs nano-filler and the 2K-WPU matrix. This indicates the existence of a complicated energy dissipating mechanism on the interfaces between CNWs and the 2K-WPU matrix (Gao et al., 2012). This mechanism can result in the variation of the properties of the nanocomposite films. The uniform distribution of the "sea-island structure" over the fractured surface indicates the well dispersion of CNWs in the 2K-WPU and demonstrates the good compatibility between the fillers and the matrix. Improved compatibility between the fillers and the matrix can be attributed to the formation of hydrogen bonds and chemical grafting between CNWs nano-filler and the 2K-WPU matrix.

3.4. Thermal properties of 2K-WPU/CNWs nanocomposite films

DSC is used to understand the interaction between CNWs nano-filler and the 2K-WPU matrix by observing the variance of domain-scale glass transition. Fig. 5 shows the DSC thermograms of 2K-WPU/CNWs nanocomposites prepared by different amounts of CNWs. The data corresponding to Fig. 5 are listed in Table 1. Unlike the long-train structure of one-component waterborne polyurethane, 2K-WPUs can form a cross-linked network after complete crosslinking reaction and result in a higher glass transition temperature (T_g). The T_g of all the 2K-WPU/CNWs nanocomposites are above 45 °C, and shift toward higher temperature with the increase of CNWs content. Change of CNWs contents from 0 to 5 wt% results in the increase of T_g from 45.1 °C to 53.3 °C. Fig. 6 shows the conceptual model explaining the T_g increase. CNWs are trapped in the cross-linked network of 2K-WPU.

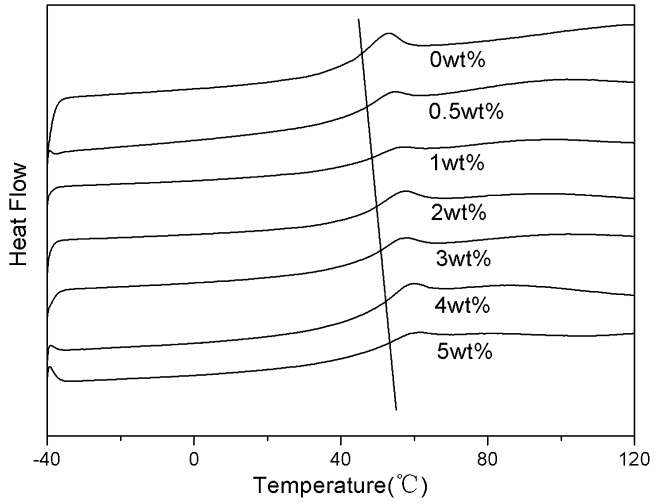

Fig. 5. DSC thermograms of 2K-WPU/CNWs nanocomposite films with different CNWs contents.

Table 1
Thermal properties of 2K-WPU/CNWs nanocomposite films.

Sample	T_g (°C)	$T_{40\%}$ (°C)
0 wt%	45.1	364.8
0.5 wt%	46.9	361.2
1 wt%	48.4	359.7
2 wt%	49.6	358.7
3 wt%	50.9	359.2
4 wt%	52.1	354.1
5 wt%	53.3	356.5

Hydrogen bonds and chemical grafting are formed between the active CNWs surface and the 2K-WPU matrix. A rigid and expanded CNWs nano-phase corresponding to the "sea-island structure" in the SEM images is formed, acting as another type of crosslinking points in the 2K-WPU matrix. As a result, the motion of polymer chains is suppressed by the rigid CNWs nano-phase, leading to the shift of T_g to high temperature.

Fig. 7 shows the TGA and the DTG curves of neat 2K-WPU (0 wt%), 2K-WPU/CNWs nanocomposites with different CNWs contents, and CNWs powder. The thermal decomposition behavior of neat 2K-WPU has been discussed in our previous work (Wu et al., 2013). Two weight loss stages are observed in the TAG curve of neat 2K-WPU. The first weight loss peak occurs around 330 °C, corresponding to the degradation of HDI tripolymer given the low

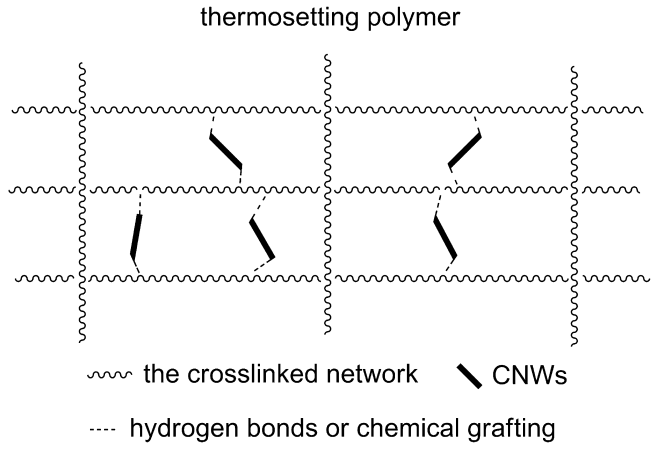

Fig. 6. Interaction model of 2K-WPU/CNWs nanocomposites.

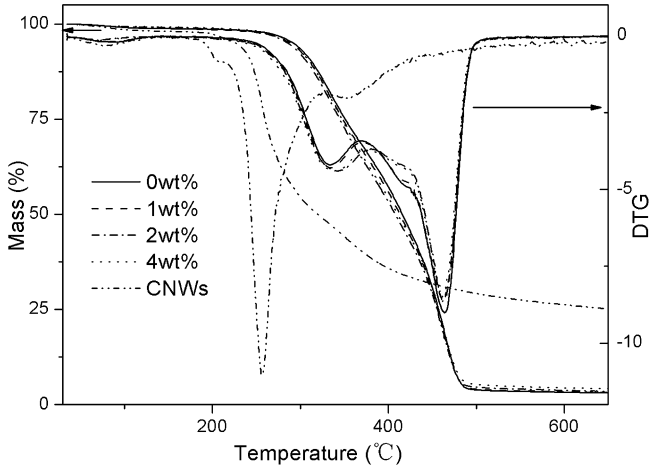

Fig. 7. TGA and DTG curves of 2K-WPU/CNWs nanocomposites with different CNWs contents and CNWs.

breaking energy of C—N bond. The second peak around 460 °C is attributed to the decomposition of TME based polyol structure. The TGA curve of CNWs reflects a typical degradation process of CNWs possessing sulfate groups arose from fiber hydrolysis with sulfuric acid (Cao, Habibi, & Lucia, 2009; Roman & Winter, 2004). In contrast to the TGA curves of CNWs, the thermograms of 2K-WPU/CNWs nanocomposites with different CNWs contents are similar to that of neat 2K-WPU. The separate degradation stage of CNWs is not observed in any TGA thermogram of 2K-WPU/CNWs nanocomposites regardless of the CNWs content. This indicates that CNWs are trapped in the cross-linked network of 2K-WPU and are completely covered by polymer chains through hydrogen bonds and chemical grafting between the active CNWs surface and the 2K-WPU matrix. The thermal degradation temperatures of 40% weight loss ($T_{40\%}$) are listed in Table 1. By comparing TGA and DTG curves at different CNWs contents, we found the addition of CNWs slightly reduce the decomposition temperature of the polymer matrix. This phenomenon was reported by researches concerning other CNWs reinforced composites (Lu & Hsieh, 2010; Ten, Turtle, Bahr, Jiang, & Wolcott, 2010). The possible explanation is that the addition of CNWs causes the increase of thermal conductivity of the material (Shimazaki et al., 2007).

3.5. Mechanical properties of 2K-WPU/CNWs nanocomposite films

Mechanical properties of 2K-WPU/CNWs nanocomposite films with different contents of CNWs were investigated by tensile testing at room temperature (about 30 °C). The results including Young's modulus (E), tensile strength (σ_b) and break elongation (ε_b) are summarized in Table 2. The E and σ_b values of all the nanocomposites show simultaneous enhancements with the increase of CNWs content. E and σ_b of 2K-WPU/CNWs nanocomposite containing 4 wt% CNWs are about 253% and 32%, respectively, higher than those of neat 2K-WPU. The modulus enhancement can be attributed to the restrained chain movement during the tensile deformation

Table 2
Mechanical properties of 2K-WPU/CNWs nanocomposite films.

Sample	E (MPa)	σ_b (MPa)	ε_b (%)
0 wt%	17.21	12.04	80.98
0.5 wt%	20.26	13.12	76.81
1 wt%	25.55	13.77	74.72
2 wt%	34.33	14.95	72.78
4 wt%	60.86	15.89	64.77

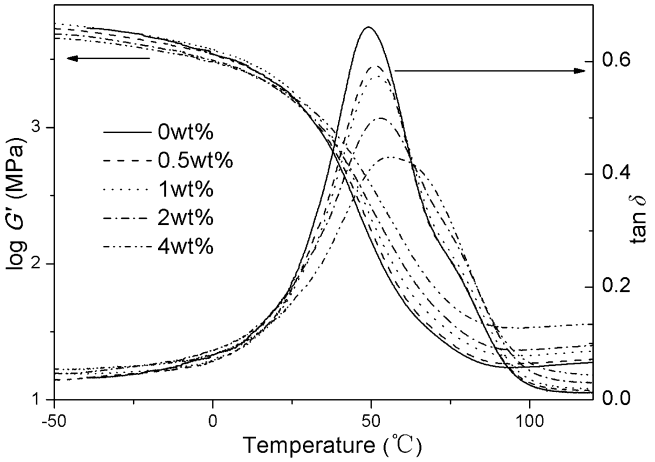

Fig. 8. DMA results of 2K-WPU/CNWs nanocomposite films with different CNWs contents.

when CNWs exist. The improvement of tensile strength indicates strong interfacial bonding between CNWs and the 2K-WPU matrix (Ten et al., 2010). However, Elongation at break of 2K-WPU/CNWs nanocomposite films decreases with the increase of CNWs content. The ε_b of nanocomposite containing 4 wt% CNWs is about 20% lower than that of neat 2K-WPU. The decrease of elongation can be attributed to the restriction of polymer segments, which is caused by the formation of a rigid CNWs nano-phase (the "sea-island structure" in the SEM images) and the microphase separation between the CNWs nano-filler and the 2K-WPU matrix.

The dynamic mechanical properties including the storage modulus (G') and the loss factor ($\tan\delta$) of 2K-WPU/CNWs nanocomposite films with different CNWs contents are shown in Fig. 8. The α-relaxation temperature (T_α), temperature at which $\tan\delta$ passed through the maximum, corresponds to the main mechanical relaxation associated with the glass transition of the polymers. Similar to T_g results from DSC tests (see Table 1), T_α shifts to higher temperature with the increase of CNWs content. The increase of T_α and the decrease of the intensity of $\tan\delta$ peaks suggest that the energy dissipation process is slowed down by the nano-fillers (Chen et al., 2008). This means the interactions between the matrix and the CNWs nano-phases become stronger with the increase of CNWs content. The molecular mobility of the chains is therefore decreased.

Variation trends of the storage modulus (G') curves of 2K-WPU/CNWs nanocomposites with different CNWs contents are similar to that of neat 2K-WPU. At low temperature (below 0 °C), the matrix is in glassy state and G' remains roughly constant. A rapid decrease of G' can be observed when the temperature gets close to T_α, corresponding to the glass transition. At temperature above T_α, the G' values of 2K-WPU/CNWs nanocomposites increase significantly with the increase of CNWs content, which is in good agreement with the results obtained from rotational rheometer measurements. These variation trends of G' can be explained as follow: G' of the matrix decreases significantly due to the movement of the chains promoted by high temperature, while CNWs nano-phase acting as another type of crosslinking points in the 2K-WPU matrix could restrain the motion of the polymers through its interaction with the chains, and recover the modulus. However, at the low temperature when the matrix is in the glassy state, the enhancement of G' of the 2K-WPU by adding CNWs is not clear. On one hand, the motions of the chains are largely restricted in the glassy state, and therefore to further restrain the motion with CNWs becomes difficult and indistinct. On the other hand, accurate determination of the glassy modulus is difficult because of its dependence on the sample dimensions (Matos Ruiz, Cavaille, Dufrense, Gerard, & Graillat, 2000). Error of the sample thickness can lead to three times higher uncertainty on the glassy modulus values (Etienne, Cavaille, Perez, Point, & Salvia, 1982).

4. Conclusion

New thermoset nanocomposites with uniform distribution of CNWs in a biomass-based 2K-WPU matrix and significant reinforcement have been prepared by low loading level CNWs and interactions between CNWs nano-filler and the polymer matrix. The viscosity of 2K-WPU dispersion increased with the addition of CNWs duo to the formation of more hydrogen bonds. Strong interactions between the matrix and CNWs nano-phases resulting to restrained molecular mobility of polymer chains and higher T_g of polymers were confirmed by both DSC and DMA tests. Mechanical properties of 2K-WPU/CNWs nanocomposites were investigated by tensile testing. The Young's modulus and tensile strength of the nanocomposite containing 4 wt% CNWs are about 253% and 32%, respectively, higher than those of neat 2K-WPU. Both rotational rheometer and DMA tests demonstrated a significantly increase of the storage modulus of the nanocomposites with the increase of CNWs content at temperature above T_α. These results indicate that CNWs exhibit excellent reinforcement effect on 2K-WPU matrix, due to the strong interactions resulting from the formation of hydrogen bonds and chemical grafting between CNWs nano-filler and the 2K-WPU matrix.

Acknowledgment

The authors gratefully acknowledge the financial support from the National Natural Science Foundation of China (contract grant number: 31100428).

References

Abdul Khalil, H. P. S., Bhat, A. H., & Ireana Yusra, A. F. (2012). Green composites from sustainable cellulose nanofibrils: A review. *Carbohydrate Polymers*, *87*, 963–979.
Akbarian, M., Olya, M. E., Ataeefard, M., & Mahdavian, M. (2012). The influence of nanosilver on thermal and antibacterial properties of a 2K waterborne polyurethane coating. *Progress in Organic Coatings*, *75*, 344–348.
Alexandre, M., & Dubois, P. (2000). Polymer-layered silicate nanocomposites: Preparation, properties and uses of a new class of materials. *Materials Science and Engineering*, *28*, 1–63.
Azizi Samir, M. A. S., Alloin, F., & Dufresne, A. (2005). Review of recent research into cellulosic whiskers, their properties and their application in nanocomposite field. *Biomacromolecules*, *6*, 612–626.
Bondeson, D., Mathew, A., & Oksman, K. (2006). Optimization of the isolation of nanocrystals from microcrystalline cellulose by acid hydrolysis. *Cellulose*, *13*, 171–180.
Cao, X. D., Dong, H., & Li, C. M. (2007). New nanocomposite materials reinforced with flax cellulose nanocrystals in waterborne polyurethane. *Biomacromolecules*, *8*, 899–904.
Cao, X. D., Habibi, Y., & Lucia, L. A. (2009). One-pot polymerization, surface grafting, and processing of waterborne polyurethane-cellulose nanocrystal nanocomposites. *Journal of Materials Chemistry*, *19*, 7137–7145.
Çetin, N. S., Tingaut, P., Ozmen, N., Henry, N., Harper, D., Dadmun, M., et al. (2009). The acetylation of cellulose nanowhiskers with vinyl acetate under moderate conditions. *Macromolecular Bioscience*, *9*, 997L 1003.
Chang, C. W., & Lu, K. T. (2012). Natural castor oil based 2-package waterborne polyurethane wood coatings. *Progress in Organic Coatings*, *75*, 435–443.
Chen, G. J., Wei, M., Chen, J. H., Huang, J., Dufresne, A., & Chang, P. R. (2008). Simultaneous reinforcing and toughening: New nanocomposites of waterborne polyurethane filled with low loading level of starch nanocrystals. *Polymer*, *49*, 1860–1870.
Eichorn, S. J., Dufresne, A., Aranguren, M., Marcovitch, N. E., Capadona, J. R., Rowan, S. J., et al. (2010). Review: Current international research into cellulose nanofibres and nanocomposites. *Journal of Materials Science*, *45*, 1–33.
Etienne, S., Cavaille, J. Y., Perez, J., Point, R., & Salvia, M. (1982). Automatic system for analysis of micromechanical properties. *Review of Scientific Instruments*, *53*, 1261–1266.
Favier, V., Chanzy, H., & Cavaille, J. Y. (1995). Polymer nanocomposites reinforced by cellulose whiskers. *Macromolecules*, *28*, 6365–6367.

Gao, Z. Z., Peng, J., Zhong, T. H., Sun, J., Wang, X. B., & Yue, C. (2012). Biocompatible elastomer of waterborne polyurethane based on castor oil and polyethylene glycol with cellulose nanocrystals. *Carbohydrate Polymers*, *87*, 2068–2075.

Ge, Z., & Luo, Y. J. (2013). Synthesis and characterization of siloxane-modified two-component waterborne polyurethane. *Progress in Organic Coatings*, *76*, 1522–1526.

Habibi, Y., Goffin, A. L., Schiltz, N., Duquesne, E., Dubois, P., & Dufresne, A. (2008). Bionanocomposites based on poly(e-caprolactone)-grafted cellulose nanocrystals by ring-opening polymerization. *Journal of Materials Chemistry*, *18*, 5002–5010.

Hubbe, M. A., Rojas, O. J., Lucia, L. A., & Sain, M. (2008). Cellulosic nanocomposites: A review. *Bioresources*, *3*, 929–980.

Jacob, M., & Thomas, S. (2008). Review: Biofibres and biocomposites. *Carbohydrate Polymers*, *71*, 353–364.

Klemm, D., Kramer, F., Moritz, S., Lindstrom, T., Ankerfors, M., Gray, D., et al. (2011). Nanocelluloses: A new family of nature-based materials. *Angewandte Chemie*, *50*, 5438–5466.

Lee, S. J., & Kim, B. K. (2012). Covalent incorporation of starch derivative into waterborne polyurethane for biodegradability. *Carbohydrate Polymers*, *87*, 1803–1809.

Lu, P., & Hsieh, Y. L. (2010). Preparation and properties of cellulose nanocrystals: Rods, spheres and network. *Carbohydrate Polymers*, *82*, 329–336.

Matos Ruiz, M., Cavaille, J. Y., Dufrense, A., Gerard, J. F., & Graillat, C. (2000). Processing and characterization of new thermoset nanocomposites based on cellulose whiskers. *Composite Interfaces*, *7*, 117–131.

Matos Ruiz, M., Cavaille, J. Y., Dufrense, A., Graillat, C., & Gerard, J. F. (2001). New waterborne epoxy coatings based on cellulose nanofillers. *Macromolecular Symposium*, *169*, 211–222.

Melchiors, M., Sonntag, M., & Kobusch, C. (2000). Recent developments in aqueous two-component polyurethane (2K-PUR) coatings. *Progress in Organic Coatings*, *40*, 99–109.

Oliveira Patricio, P. S., Miranda, I. P., Silva, N. C. F., Ayres, E., Pereira, F. V., & Orefice, R. L. (2013). Tailoring the morphology and properties of waterborne polyurethanes by the procedure of cellulose nanocrystal incorporation. *European Polymer Journal*, *49*, 3761–3769.

Otts, D. B., Pereira, K. J., Arret, W. L., & Urban, M. W. (2005). Dynamic colloidal processes in waterborne two-component polyurethane and their effects on solution and film morphology. *Polymer*, *46*, 4776–4788.

Otts, D. B., & Urban, M. W. (2005). Heterogeneous crosslinking of waterborne two-component polyurethanes; stratification processes and the role of water. *Polymer*, *46*, 2699–2709.

Pu, Y., Zhang, J., Elder, T., Deng, Y., Gatenholm, P., & Ragauskas, A. J. (2007). Investigation into nanocellulosics versus acacia reinforced acrylic films. *Composites: Part B*, *38*, 360–366.

Qua, E. H., Hornsby, P. R., Sharma, H. S. S., Lyons, G., & McCall, R. D. (2009). Preparation and characteristics of poly(vinyl alcohol) nanocomposites made from cellulose nanofibers. *Journal of Applied Polymer Science*, *113*, 2228–2247.

Roman, M., & Winter, W. T. (2004). Effect of sulfate groups from sulfuric acid hydrolysis on the thermal degradation behavior of bacterial cellulose. *Biomacromolecules*, *5*, 1671–1677.

Roohani, M., Habibi, Y., Belgacem, N. M., Ebrahim, G., Karimi, A. N., & Dufresne, A. (2008). Cellulose whiskers reinforced polyvinyl alcohol copolymers nanocomposites. *European Polymer Journal*, *44*, 2489–2498.

Shimazaki, Y., Miyazaki, Y., Takezawa Masaya Nogi, M., Abe, K., Ifuku, S., & Hiroyuki Yano, H. (2007). Excellent thermal conductivity of transparent cellulose nanofiber/epoxy resin nanocomposites. *Biomacromolecules*, *8*, 2976–2978.

Siqueira, G., Bras, J., & Dufresne, A. (2010). New process of chemical grafting of cellulose nanoparticles with a long chain isocyanate. *Langmuir*, *26*, 402–411.

Souza Lima, M. M., & Borsali, R. (2004). Rodlike cellulose microcrystals: Structure, properties, and applications. *Macromolecular Rapid Communications*, *25*, 771–787.

Stenstad, P., Andresen, M., Tanem, B. S., & Stenius, P. (2008). Chemical surface modifications of microfibrillated cellulose. *Cellulose*, *15*, 35–45.

Ten, E., Turtle, J., Bahr, D., Jiang, L., & Wolcott, M. (2010). Thermal and mechanical properties of poly(3-hydroxybutyrate-co-3-hydroxyvalerate)/cellulose nanowhiskers composites. *Polymer*, *51*, 2652–2660.

Wicks, Z., Wicks, D., & Rosthauser, J. (2002). Two package waterborne urethane systems. *Progress in Organic Coatings*, *44*, 161–183.

Wu, G. M., Kong, Z. W., Chen, C. F., Chen, J., Huo, S. P., & Jiang, J. C. (2013). Crosslinking reaction and properties of two-component waterborne polyurethane from terpene-maleic ester type epoxy resin. *Journal of Applied Polymer Science*, *128*, 132–138.

Wu, G. M., Kong, Z. W., Chen, J., & Jiang, J. C. (2011). Preparation and properties of nonionic polyol dispersion from terpinene-maleic ester-type epoxy resin. *Journal of Applied Polymer Science*, *120*, 579–585.

Wu, G. M., Kong, Z. W., Huang, H., Chen, J., & Chu, F. X. (2007). Synthesis of epoxy resin from hydrogenated terpinene-maleic anhydride. *Chemistry & Industry of Forest Products*, *27*, 57–62.

Zou, J. W., Zhang, F., Huang, J., Chang, P. R., Su, Z. M., & Yu, J. H. (2011). Effects of starch nanocrystals on structure and properties of waterborne polyurethane-based composites. *Carbohydrate Polymers*, *85*, 824–831.